Crystal Structure and Physical Properties of {Bis(ethylenedithio)tetrathiafulvalene}$_2$dicyano-Silver and -Gold

Mohamedally Kurmoo,*,# Peter Day, Tadaoki Mitani,† Hiroshi Kitagawa,† Hideo Shimoda,† Den Yoshida,† Philippe Guionneau,†† Yvette Barrans,†† Daniel Chasseau,†† and Laurent Ducasse†††

The Royal Institution of Great Britain, 21 Albemarle Street,London WIX 4BS, UK

†Japan Institute of Science and Technology, 15 Asahidai, Tatsunokuchi, Ishikawa 923-12

††Laboratoire de Cristallographie et de Physique Cristalline, CNRS, URA 144, Universite Bordeaux 1, 33405 Talence Cedex, France

†††Laboratoire de Physico-Chimie Theorique, CNRS, ERS 133, Universite Bordeaux 1, 33405 Talence Cedex, France

(Received December 4, 1995)

We report the crystal and electronic band structures and the electrical, magnetic, and optical properties of {bis(ethylenedithio)tetrathiafulvalene}$_2$dicyano-silver and -gold, η-(BEDT–TTF)$_2$M(CN)$_2$, M = Ag or Au. The compounds belong to the monoclinic system; space group $C2/c$, $a = 36.28(8)$, $b = 4.286(2)$, $c = 22.02(6)$ Å, $\beta = 110.62(9)°$ and $V = 3205$ Å^3, and $a = 36.44(8)$, $b = 4.256(2)$, $c = 22.16(6)$ Å, $\beta = 111.3(1)°$ and $V = 3201$ Å^3, respectively. The structure consists of pairs of stacks with parallel BEDT–TTF molecules along b. Molecules in neighboring pairs of stacks are tilted by 55.3°. There are several short S···S contacts between stacks to form layers, which are separated by the anions along a. The transfer integrals suggest a highly dimerized system. The band structure calculation, however, predicts metallic behavior contrary to the semiconducting properties observed ($\sigma_{RT} \approx 10^{-1}$—10 S cm^{-1} and $E_A = 0.15(2)$ eV). The static (SQUID magnetometry) and spin (EPR) susceptibilities are modelled to a singlet–triplet system with an energy gap of 315(5) K (39(1) meV). This is one of two phases in the BEDT–TTF family to exhibit an activated susceptibility for a spin dimer model.

The multi-phasic nature of molecular materials can be of great importance in obtaining different physical properties but can at the same time be a big handicap when the phases are not physically separable (intergrown) or they have the similar crystal morphologies. The control of crystal growth of single phases is better documented for high-temperature synthesis than for the electrochemical method used to crystallize organic conductors and superconductors. In general, for the latter several phases are grown at the same time and under the same experimental conditions.[1] On the other hand, no evidence of intergrowth of different phases have been observed though in some cases the unit cell dimensions are sufficiently close to allow such a problem to arise. Given the lamellar structure of these compounds it is possible that misfits of different BEDT–TTF layers may form. The latter may be less ordered so that their crystal structure have not been closely looked at. Another problem is that several of the crystal phases are isomorphous and thus other methods of identification, for example IR, EPR, and X-ray analysis, are required. Among the charge-transfer salts of the BEDT–TTF family [BEDT–TTF = bis(ethylenedithio)-tetrathiafulvalene], the triiodide anion has produced more than ten crystal phases;[2] and seven phases for $[Ag(CN)_2]^-$,[3] while for $[Au(CN)_2]^-$ only two phases have been identified, which have isostructural silver analogues.[4—6] One of the latter (η-phase) with $M(CN)_2^-$, M = Ag or Au, is the subject of the present paper. We will describe their crystal structures, results of band structure calculations, and the electrical, magnetic, and optical properties. The crystal structure of the gold derivative has previously been reported.[4]

Due to very slight differences in the crystal structures of salts of the BEDT–TTF family, several ground states can be found: Localized and delocalized systems which display semiconducting, metallic, and superconducting electrical properties and Pauli paramagnetic, low dimensional (1D- and 2D-) antiferromagnetic and 3D-ordered (antiferromagnetic and weak ferromagnetic).[2] Charge-transfer salts of BEDT–TTF with $[Ag(CN)_2]^-$ embrace all these properties except for a ferromagnetic ground state.[3,6] Such a range of behaviors arises from the variety of crystal packing motifs and electronic band structures. The present compounds fall in the semiconducting category as Mott–Hubbard systems with the number of spins equivalent to the number of $(BEDT–TTF)_2^+$ sites. The temperature dependence of the magnetic susceptibility is that expected for a Singlet–Triplet model. We discuss some trends in the structure-property

#Present address: Institut de Physique et Chimie des Matériaux de Strasbourg, Groupe des Matériaux Inorganiques, 23 rue du Loess, F-67037 Strasbourg Cedex, France.

relationships for compounds with linear anions.

Experimental

Synthesis. BEDT–TTF, prepared by the method of Larsen and Lenoir,[7] was recrystallized twice from chloroform before use. $[(C_4H_9)_4N]M(CN)_2$, M = Ag or Au was prepared as colorless crystals by metathesis of $[(C_4H_9)_4N]NO_3$ and $K[M(CN)_2]$ in distilled water. Recrystallization was carried out in minimum volume of absolute ethanol. The purity of BEDT–TTF and the electrolyte were checked by chemical analysis. The charge-transfer salt was obtained by electrocrystallization of BEDT–TTF in CH_2Cl_2 containing the anion. A three compartment cell equipped with platinum wire (1 mm) electrodes was used, with a constant applied current of 0.5—1 μA. The crystals were highly reflecting black plates of maximum dimension $2\times1\times0.1$ mm^3.

X-Ray Crystallography. All the crystals appear single under the microscope and the first crystal of each compound chosen for crystallography gave single Bragg reflections in Laue and Weissenberg photographs. This is quite rare for this class of materials. Data collection was performed at room temperature using a Nonius CAD-4 diffractometer with graphite monochromatized Mo $K\alpha$ (λ = 0.71069 Å) radiation. The unit cell parameters were obtained from accurately measured angles of 25 intense reflections. Three reflections were monitored hourly and no large variation of intensity or position was observed. Data were corrected for Lorentz, polarization and absorption. More details are given in Table 1. Data were collected and analyzed for both compounds; the unit cell dimensions and its crystal structure of the $[Au(CN)_2]^-$ salt was found to correspond to those reported by Amberger et al.[4] and thus will not be reported here. Those of the $[Ag(CN)_2]^-$ salt is unknown and thus full details of its crystal structure and comparison with the isostructural $[Au(CN)_2]^-$ will be given.

The structure of the $[Ag(CN)_2]^-$ salt was solved by direct methods using the package MITHRIL.[8] The hydrogen atoms were placed in theoretical positions (C–H, 1 Å) and refined isotropically in the final cycles. The carbon, sulfur, silver, and nitrogen atoms were refined anisotropically. The atomic positions and isotropic or anisotropic thermal factors were obtained by the least-squares method using 190 parameters to a final R = 0.033, R_w = 0.033, and S = 0.97. Difference Fourier maps at the end of the refinement give residual electron density of less than ±0.5 e Å^{-3}. Further details are listed in Table 1.

Transfer Integrals and Band Structure Calculation. The transfer integrals, band structure, and Fermi surface of η-(BEDT–TTF)$_2$[Ag(CN)$_2$] have been calculated within the semiempirical extended Hückel theory[9] using a double-ζ basis set and tight binding.[10]

Electrical Transport. DC resistivity measurements were made along the three crystallographic axes with applied current of 0.1 or 1 μA. The contacts were made with 25 μm gold wire and gold paste. The temperature was measured by a calibrated Pt–Co resistor; the sample and the sensor were thermally anchored to a copper block surrounded by helium exchange gas.

Electron Spin Resonance. Spectra were collected on single crystals by use of a JEOL-RE3X spectrometer operating in a TE_{011} mode at 9 GHz and 100 KHz field modulation. Frequency was measured by an Advantest R5372 counter. Temperature of the sample was measured by a Au–Fe (0.07%)/chromel thermocouple by use of an APD cryogenics continous flow cryostat and a Lakeshore 330 controller. Crystals were mounted on a cut flat face of 3 mm diameter Teflon® rods using a smear of silicone grease, which was then placed in a quartz tube containing helium exchange gas. A manganese marker and a TEMPOL sample were used to calibrate the magnetic field and g-values.

Table 1. Crystal and Refinement Data for η-(BEDT–TTF)$_2$-[Ag(CN)$_2$] at 295 K

Chemical formula	$C_{22}H_{16}N_2S_{16}Ag$
M_r	928
Crystal system	Monoclinic
Spece group	$C2/c$
Unit cell dimensions: a/Å	36.28(8)
b/Å	4.286(2)
c/Å	22.02(6)
β/°	110.62(9)
V/Å^3	3205
D_c/g cm^{-3}	2.111
Z	4
F(000)	1988
Crystal Dimensions/mm	$0.05\times0.175\times0.275$
μ/cm^{-1}	57.61
Data collection and Processing:	
Diffractometer	CAD-4
X-Ray radiation	Mo $K\alpha$
λ/Å	0.71069
Scan mode, θ_{max}	$\omega/2\theta$, 28°
Min–Max h, k, l	(−48, 0, −1)–(48, 5, 29)
No. of standard reflections	3
Variation/%	1.5
No. of reflections:	
Total	4698
Unique (R_{int}/%)	2445, (1.4)
Observed	2304
Absorption correction	Empirical
T_{min}, T_{max} correction	0.809, 1.000
Structural analysis and refinement:	
No. of parameters	190
criteria, Weighting scheme	$I\geq3\sigma(I)$, $w=1/[\sigma^2+0.005F^2]$
R (observed data)/%	3.3
R_w (observed data)/%	3.3
S, $(\Delta/\sigma)_{max}$	0.97, 0.001
Δr_{min}, Δr_{max}/eÅ^{-2}	−0.44, +0.37

Static Magnetic Susceptibility. Data were recorded on cooling and warming using a MPMS-7 SQUID magnetometer in fields ranging from 100 G to 1 Tesla. The data were corrected for the core diamagnetism estimated from the sum of Pascal constants amounting to -4.42×10^{-4} emu mol^{-1}.

Optical Reflectivity. Mid-infrared reflectivity data of single crystals were recorded at room temperature by use of a Perkin–Elmer 1710 spectrometer in conjunction with an IR-PLAN microscope. A KRS5 polarizer was used to align the electric vector of the IR beam parallel to the b and c axes respectively.

Results

Crystal Structure. η-(BEDT–TTF)$_2$[Ag(CN)$_2$] crystallizes in the monoclinic system; space group $C2/c$, a = 36.28(8), b = 4.286(2), c = 22.02(6) Å, β = 110.62(9)°, and V = 3205 Å^3. It is isostructural to the gold analogue, a = 36.44(8), b = 4.256(2), c = 22.16(6) Å, β = 111.3(1)°, and V = 3201 Å^3. These values are similar to those reported by Amberger et al.,[4] a = 36.517(7), b = 4.254(1), c = 22.117(4)

Å, $\beta = 111.38(2)°$, and $V = 3199$ Å^3. The rectangular plate crystals have the short and long axes of the large face corresponding to the crystallographic *b* and *c* axes, respectively. The asymmetric unit contains one BEDT–TTF molecule and one half of $[Ag(CN)_2]^-$, i.e., half a formula unit; the unit cell (Fig. 1), generated by symmetry corresponding to the *C*2/*c* space group, contains four formula units of (BEDT–TTF)$_2$[Ag(CN)$_2$].## The atomic coordinates, bond lengths, and angles are given in Tables 2 and 3.

The structure consists of stacks of planar BEDT–TTF (Fig. 2) molecules along *b* separated by $[Ag(CN)_2]^-$ at every half cell along the *a* direction. The stacks are pair-wise with the plane of the molecules of one pair parallel and molecules from different pairs make a dihedral angle of 55.3°. This angle is 53.2° in η-(BEDT–TTF)$_2$[Au(CN)$_2$]. There are

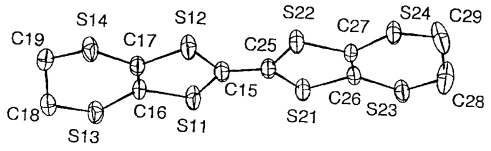

Fig. 1. Labelling scheme adopted for the BEDT–TTF molecule with thermal ellipsoids (50% probability) of the atoms in η-(BEDT–TTF)$_2$[Ag(CN)$_2$].

##The labelling scheme adopted, atomic coordinates, interatomic distances, angles, and observed and calculated structure factors have been deposited as supplementary materials at the Cambridge Crystallographic Data Base.

Table 2. Fractional Atomic Coordinates and Thermal Factors for η-(BEDT–TTF)$_2$[Ag(CN)$_2$] at 295 K

Atom	*x*	*y*	*z*	B_{eq}/Å^2
Ag(1)	0.5000	0.5000	0.5000	5.49(3)
C(2)	0.5082(1)	0.730(1)	0.4246(2)	4.5(3)
N(3)	0.5133(1)	0.850(1)	0.3822(2)	5.6(2)
S(11)	0.22611(3)	0.1758(3)	0.17075(5)	3.19(5)
S(12)	0.22624(3)	0.4774(4)	0.05118(5)	3.22(5)
S(13)	0.14044(3)	0.1740(3)	0.13531(5)	3.05(5)
S(14)	0.14077(3)	0.5181(4)	−0.00990(5)	3.36(5)
C(15)	0.2535(1)	0.334(1)	0.1274(2)	2.5(2)
C(16)	0.18046(9)	0.273(1)	0.1128(2)	2.3(2)
C(17)	0.1805(1)	0.407(1)	0.0576(2)	2.4(2)
C(18)	0.1006(1)	0.364(1)	0.0717(2)	3.4(2)
C(19)	0.1011(1)	0.315(1)	0.0043(2)	3.4(2)
S(21)	0.32156(3)	0.1748(3)	0.22529(5)	2.87(5)
S(22)	0.32038(2)	0.4954(4)	0.10699(5)	3.05(5)
S(23)	0.40793(3)	0.1761(3)	0.28803(5)	3.17(5)
S(24)	0.40589(3)	0.5571(3)	0.14558(5)	3.10(5)
C(25)	0.29359(9)	0.337(1)	0.1507(2)	2.4(2)
C(26)	0.36715(9)	0.282(1)	0.2207(2)	2.5(2)
C(27)	0.36642(9)	0.425(1)	0.1661(2)	2.4(2)
C(28)	0.4471(1)	0.363(1)	0.2710(2)	4.9(3)
C(29)	0.4460(1)	0.367(1)	0.2058(2)	4.8(3)

Table 3. Bond Lengths and Angles of η-(BEDT–TTF)$_2$[Ag(CN)$_2$] at 295 K

Bond lengths	Ag(1)	C(2)	2.041	Bond angles	Ag(1)	C(2)	N(3)	177.9
	C(2)	N(3)	1.137(8)		C(15)	S(11)	C(16)	94.8(2)
	S(11)	C(15)	1.740(5)		C(15)	S(12)	C(17)	95.5(2)
	S(11)	C(16)	1.748(4)		C(16)	S(13)	C(18)	100.8(2)
	S(12)	C(15)	1.731(5)		C(17)	S(14)	C(19)	101.1(2)
	S(12)	C(17)	1.741(4)		S(11)	C(15)	S(12)	115.4(2)
	S(13)	C(16)	1.744(4)		S(11)	C(15)	C(25)	122.4(3)
	S(13)	C(18)	1.813(5)		S(12)	C(15)	C(25)	122.2(3)
	S(14)	C(17)	1.734(4)		S(11)	C(16)	S(13)	113.8(2)
	S(14)	C(19)	1.801(5)		S(11)	C(16)	C(17)	117.3(3)
	C(15)	C(25)	1.362(6)		S(13)	C(16)	C(17)	128.8(3)
	C(16)	C(17)	1.345(6)		S(12)	C(17)	S(14)	114.3(2)
	C(18)	C(19)	1.505(7)		S(12)	C(17)	C(16)	116.9(3)
	S(21)	C(25)	1.743(5)		S(14)	C(17)	C(16)	128.8(3)
	S(21)	C(26)	1.752(4)		S(13)	C(18)	C(19)	114.6(3)
	S(22)	C(25)	1.729(5)		S(14)	C(19)	C(18)	113.1(3)
	S(22)	C(27)	1.745(4)		C(25)	S(21)	C(26)	95.2(2)
	S(23)	C(26)	1.745(4)		C(25)	S(22)	C(27)	95.4(2)
	S(23)	C(28)	1.781(6)		C(26)	S(23)	C(28)	101.9(2)
	S(24)	C(27)	1.741(4)		C(27)	S(24)	C(29)	100.9(2)
	S(24)	C(29)	1.784(6)		C(15)	C(25)	S(21)	122.9(3)
	C(26)	C(27)	1.343(6)		C(15)	C(25)	S(22)	121.9(3)
	C(28)	C(29)	1.424(8)		S(21)	C(25)	S(22)	115.2(2)
					S(21)	C(26)	S(23)	114.8(2)
					S(21)	C(26)	C(27)	116.7(3)
					S(23)	C(26)	C(27)	128.5(3)
					S(22)	C(27)	S(24)	114.1(2)
					S(22)	C(27)	C(26)	117.3(3)
					S(24)	C(27)	C(26)	128.5(3)
					S(23)	C(28)	C(29)	118.4(4)
					S(24)	C(29)	C(28)	118.8(4)

several short S···S contacts with molecules in neighboring stacks along c to form layers.

The thermal parameters of the BEDT–TTF molecule are almost uniform, unlike those of most salts in this family which become progressively larger from the center of the molecules to the H_2C–CH_2 ends. The only disordered atoms are those on the ethylene group on one side of the molecule (Fig. 1). The B_{eq}'s of C(28) and C(29) are about 40% larger than the average of the rest of the atoms. This results in a shorter bond length (1.42 Å) and wider angles (118.6°) than expected (1.50 Å and 115°). We note that the sulfur atoms vibrate more than the carbon atoms. The thermal parameters of the atoms of the anion are larger than the BEDT–TTF molecule as also observed in some other compounds of BEDT–TTF.

Since there is only one independent BEDT–TTF molecule and in the stacking direction the unit cell is only one molecule thick, there is only one mode of overlap along the stacking axis, which is not the most common bond-over-ring type (Fig. 3).[2b] We define the overlap by three parameters, Δx: the shift of one molecule with respect to the reference molecule along the short axis of the BEDT–TTF molecule (1.95 Å), Δy: that along the long axis (0.47 Å), and Δz: the average distance between the molecules (3.82 Å), calculated from the mean plane defined by the four inner sulfur atoms and the two central carbon atoms. These distances would indicate that intermolecular overlap is too small for high electrical conductivity (see band structure calculation below). To achieve metallic conductivity, bond-over-ring overlap and a regular spacing between molecules (ca. 3.6 Å) are advantageous as for β-(BEDT–TTF)$_2$AuI$_2$,[11] while a shorter distance usually results in localization through dimerization as shown for (BEDT–TTF)$_2$GaCl$_4$ and β'-(BEDT–TTF)$_2$AuCl$_2$.[12,13] The shortest S···S distances observed between molecules in a stack are 3.988(2) Å for S(12)···S(11)* and 3.897(2) Å for S(22)···S(21)*; they are longer than the sum of the van der Waals ionic radii of the sulfur atoms. In contrast, the S···S distances between molecules in different stacks are shorter and less than the sum of the van der Waal radii. Interaction modes between neighboring molecules are defined in Fig. 4. Between those defined by interaction **I1**, S(14)···S(22)* = 3.609(2) Å and S(14)···S(24)* = 3.398(2) Å; **I2**, S(14)···S(22)* = 3.677(2) and **I5**, S(13)···S(21)* = 3.599(2) Å and S(13)···S(23)* = 3.556(2) Å. These distances are similar to those found in the gold derivative.

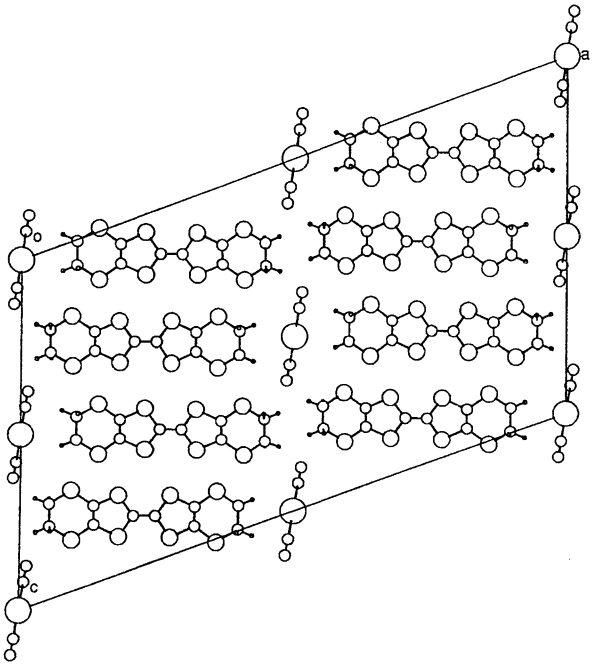

Fig. 2. View of the unit cell of η-(BEDT–TTF)$_2$[Ag(CN)$_2$] along b^*.

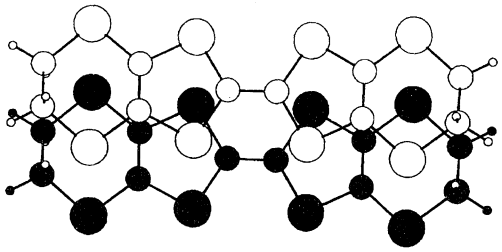

Fig. 3. Mode of overlap of the BEDT–TTF molecules along the b-axis.

The bond lengths of the BEDT–TTF molecule are consistent with a charge of 0.5+ per molecule as expected from the stoichiometry. The C=C bond length is 1.361 Å and the averaged C–S is 1.736 Å.[14] The [Ag(CN)$_2$]$^-$ is almost linear with bond lengths similar to those observed for other [Ag(CN)$_2$]$^-$ salts of BEDT–TTF. There is one short anion–cation distance (3.436 Å, S···N) in η-(BEDT–TTF)$_2$[Ag(CN)$_2$], which is even shorter (3.313 Å) in η-(BEDT–TTF)$_2$[Au(CN)$_2$], possibly as a result of the smaller dihedral angle between the molecules of adjacent stacks.

Band Structure. The values of the intermolecular transfer integrals are indicated in Fig. 4. The intrastack transfer integral is small (−21 meV) compared to those between stacks (ca. 65 and 214 meV). These values reflect the distances between molecules within a stack and those between

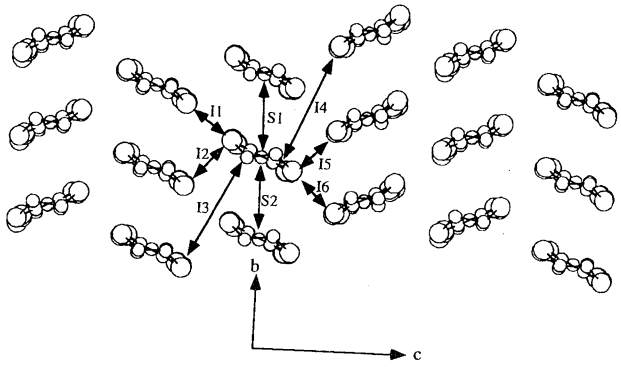

Fig. 4. View of the layer of η-(BEDT–TTF)$_2$[Ag(CN)$_2$] along C=C bond, giving the calculated transfer integrals (meV) between neighboring molecules [S1 = S2 = 21, I1 = −68, I2 = 214, I3 = I4 = 0, I5 = I6 = 65].

stacks. The strong alternation in transfer integrals along c (ratio of ca. 3), suggests a highly localized system, as observed for α'-(BEDT–TTF)$_2$[Ag(CN)$_2$]. This is consistent with the semiconducting behavior and the high magnetic susceptibility ($S = 1/2$, one spin per dimer) observed.

The corresponding band structure and Fermi surface are depicted in Fig. 5. The four molecules in one layer in the unit cell lead to four bands which are 3/4 filled. The dispersion of the upper two bands results in the Fermi level bisecting them. The Fermi surface thus is a dog-bone cross-sectioned cylinder similar to that found for α-(BEDT–TTF)Cd$_{0.66}$(SCN)$_2$ which has an α-type structure.[15] Such Fermi surfaces are common to several α-phase materials.[3,15] However, our calculation predicts electrical properties expected for a metal in contrast to the semiconducting behavior observed for the present compound. A similar observation was made for α-(BEDT–TTF)Cd$_{0.66}$(SCN)$_2$.[15]

Electrical Transport. Conductivity measurements on several crystals show semiconducting behavior with a room temperature conductivity in the range 10^{-1}—10 S cm^{-1} (Fig. 6) and an activation energy 0.15(2) eV. The conductivity is anisotropic. The room temperature conductivities along the most conducting axis is higher than that of α'-(BEDT–TTF)$_2$[Ag(CN)$_2$] and the activation energy is half.[16]

Electron Paramagnetic Resonance. The spectra consist of a single Lorentzian signal at all temperatures and orientations. Its g-values (2.003(1) and 2.010(1) parallel to c and a, respectively) are within the range of values observed for BEDT–TTF salts, having a charge of 0.5+ per molecule.[17] The g-value is temperature independent. The linewidth of the resonance decreases from room temperature to a minimum at ca. 70 K. At 50 K, it shows a sharp lambda-type peak

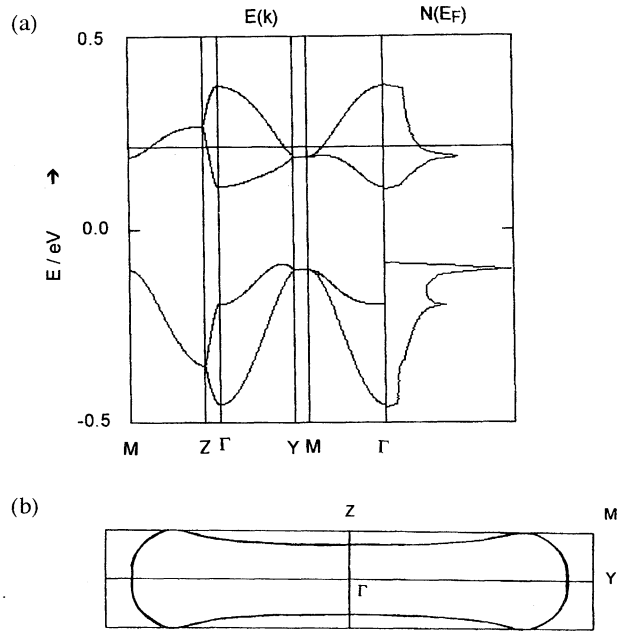

Fig. 5. Band structure of η-(BEDT–TTF)$_2$[Ag(CN)$_2$]: (a) Energy dispersion and density of states; (b) the Fermi surface.

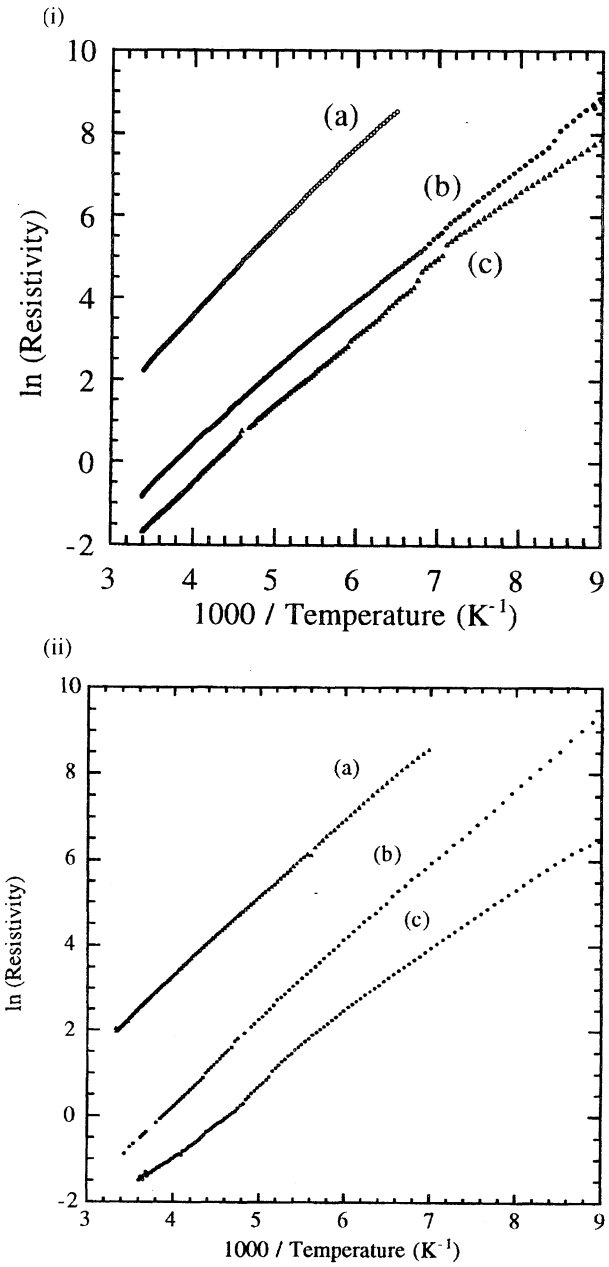

Fig. 6. Temperature dependence of the electrical resistivity along the three crystallographic axes of (i) η-(BEDT–TTF)$_2$[Ag(CN)$_2$] and (ii) η-(BEDT–TTF)$_2$[Au(CN)$_2$].

(Fig. 7). On the other hand, the intensity of the resonance does not show any anomaly at either the minimum at ca. 70 K or the sharp peak at ca. 50 K (Fig. 8). Since there is no sign of overlapping resonances, which may indicate that the low-temperature spectrum is due to an impurity, we suggest that the change in linewidth may be due to a change in regime of the relaxation process as the concentration of triplet excitons is lowered below some critical values. We note that such behavior has also been observed for (BEDT–TTF)$_2$GaCl$_4$ which again behaves as a singlet–triplet system.[12] The temperature dependence of the intensity of the resonance is the same as that observed for the static susceptibility measured

by the SQUID and thus will be discussed in the following section.

Static Susceptibility. At room temperature the molar susceptibilities of η-(BEDT–TTF)$_2$[Ag(CN)$_2$] and η-(BEDT–TTF)$_2$[Au(CN)$_2$] are 8.5×10^{-4} emu mol^{-1}. For both salts the susceptibility increases very gradually to a broad maximum of ca. 9×10^{-4} emu mol^{-1} at ca. 200 K (Fig. 9); at ca. 100 K it drops rapidly to zero at ca. 40 K. For η-(BEDT–TTF)$_2$[Au(CN)$_2$] it increases below 20 K as the inverse of temperature to ca. 2×10^{-4} emu mol^{-1} at 2 K due to a small Curie contribution equivalent to $<0.1\%$ $S=1/2$ spins. It is slightly more for η-(BEDT–TTF)$_2$[Ag(CN)$_2$]. By removing the Curie component the intrinsic susceptibility of the η-(BEDT–TTF)$_2$[M(CN)$_2$] crystals can be seen to tend to a value of zero emu mol^{-1} at temperatures below 50 K.

Optical Reflectivity. The polarized mid-infrared spectra are shown in Fig. 10. The background reflectivity is small and the vibrational part is strong. The strongest vibration is the C=C mode at 1390 cm^{-1} and the C≡N mode at 2230 cm^{-1} is weak. Several other sharp modes of medium intensity are observed at 1280, 1178, 1056, 888, 780, 684, and 490

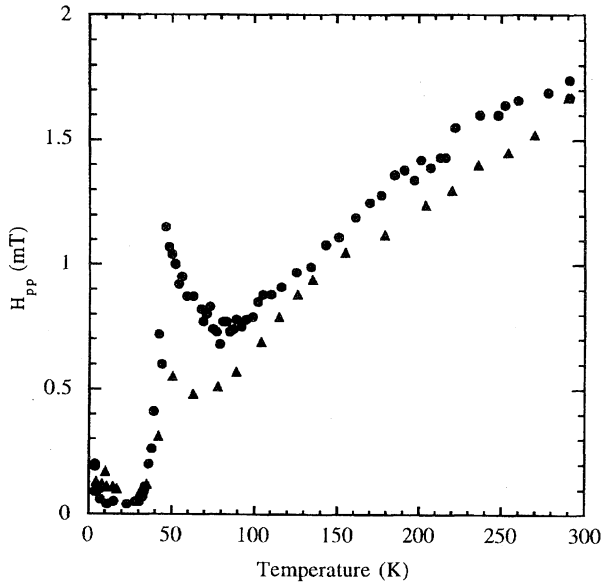

Fig. 7. Temperature dependence of the peak-to-peak linewidths of the EPR signal of η-(BEDT–TTF)$_2$[Ag(CN)$_2$] (triangles) and η-(BEDT–TTF)$_2$[Au(CN)$_2$] (circles) for $H_0//c$.

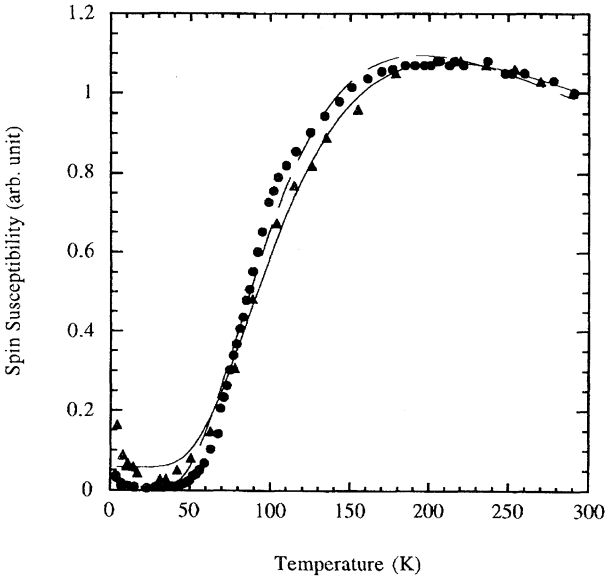

Fig. 8. Temperature dependence of the spin susceptibility of η-(BEDT–TTF)$_2$[Ag(CN)$_2$] (triangles) and η-(BEDT–TTF)$_2$[Au(CN)$_2$] (circles) and the fit to a singlet–triplet model (lines).

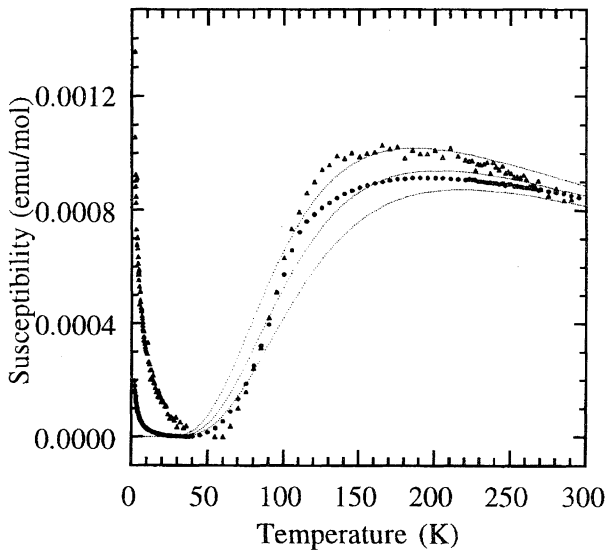

Fig. 9. Temperature dependence of the bulk magnetic susceptibility of η-(BEDT–TTF)$_2$[Ag(CN)$_2$] (triangles) and η-(BEDT–TTF)$_2$[Au(CN)$_2$] (circles). The solid lines are theoretical trace for the singlet–triplet model with $2J/k_B=300$, 325, and 350 K from top to bottom.

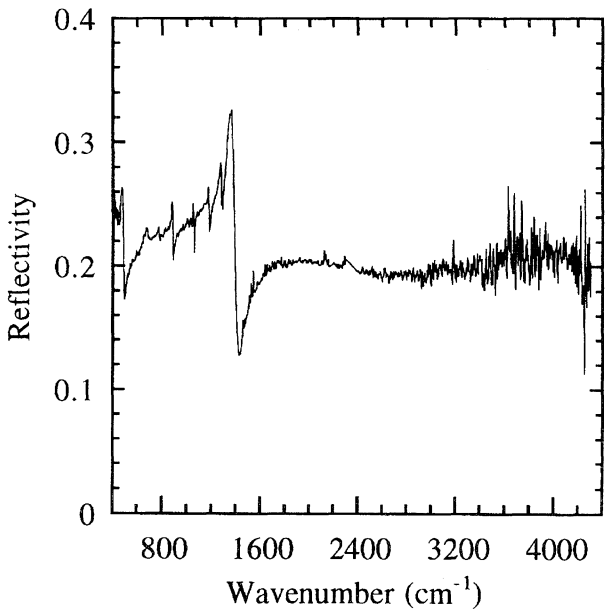

Fig. 10. Mid-infrared reflectivity of η-(BEDT–TTF)$_2$[Au(CN)$_2$].

cm^{-1}. Although the electrical measurement indicates a band gap of 0.3 eV, there is no corresponding observable optical transition in contrast to the α'-(BEDT–TTF)$_2$MX$_2$ series.[18] For a dimer the lowest energy electronic transition expected is that between the bonding and antibonding combination which is given by $2t$ (420 meV at the upper limit).

Discussion

Amongst the classes of BEDT–TTF change-transfer salts, that with linear anions has a special position, for it has provided the first isostructural series of ambient pressure superconductors from which structural correlations were drawn.[19] These anions have also provided several sets of structural phases (α-, α'-, β-, β'-, β''-, θ, $\varkappa$-, etc). Our own experience with the [Ag(CN)$_2$] anion is that a multitude of phases can be obtained (sometimes all in a one pot synthesis) indicating that the thermodynamic stabilities of the different phases are very similar. Fortunately, in the present study the η-(BEDT–TTF)$_2$M(CN)$_2$ crystals were the only product, thus allowing us to do bulk measurements. Among the seven [Ag(CN)$_2$]$^-$ salts identified to date, three have closely related structures of the α-type.[3] The variety of structural phases is thought to be due to the secondary bonding ability of the cyano group in the anion as well as being a π-acceptor. Furthermore, the ability of the silver atom to support trigonal coordination of ligands, in contrast to the case of gold is probably the reason why a $\varkappa$-phase superconductor of the latter has not been found.

The structure of η-(BEDT–TTF)$_2$[Ag(CN)$_2$] contains dimers of BEDT–TTF which give rise to alternating large intradimer and small interdimer transfer integrals along the c direction. However, molecules forming the dimers within a stack are not face-to-face but side-by-side perpendicular to the stack in contrast to that found for α'-(BEDT–TTF)$_2$[Ag(CN)$_2$].[20] Nevertheless, the band structure calculated within the extended Hückel formalism from the observed crystal structure predicts a metallic rather than the observed semiconducting behavior. The reason for this contradiction, which has been discussed previously, is that the localized electron behavior cannot be accounted for by a one-electron approach.[12]

The double-stack packing in η-(BEDT–TTF)$_2$[M(CN)$_2$][###] is similar to that found in the molecular superconductor TTF[Ni(dmit)$_2$]$_2$ {dmit = $C_5S_5^{2-}$, 1,3-dithiole-2-thione-4,5-dithiolato} with the TTF {tetrathiafulvalene} replaced by the M(CN)$_2$ anions and the Ni(dmit)$_2$ by the BEDT–TTF molecule.[21] The observed dihedral angle of the two η-(BEDT–TTF)$_2$[M(CN)$_2$] compounds would classify them as semiconductors by the correlation established previously.[3]

The magnetic susceptibilities of η-(BEDT–TTF)$_2$[M(CN)$_2$] are just slightly lower than expected for a localized one electron per dimer system (1.25×10^{-3} emu mol^{-1}). However, the values do not differ much from those found for the α'-(BEDT–TTF)$_2$X salts where X is [AuBr$_2$]$^-$ or [Ag(CN)$_2$]$^-$ or BEDT–TTF salts with a dimerized structure.[22] It is clear that there is a magnetic gap in the energy spectrum of these systems since the susceptibility tends to zero at low-temperatures. As already pointed out by several authors,[2,22] it is probable that Coulomb repulsion is large and the spins are localized with one on each BEDT–TTF dimer, consistent with the semiconducting nature of the salt. Thus, these salts may be classified as Mott–Hubbard insulators with poor π delocalization and large Coulomb repulsion between the conduction electrons as found for α'-(BEDT–TTF)$_2$X.[22]

Good agreement between observed and calculated susceptibilities can be obtained if we fit the data to a singlet–triplet model:[23]

$$\chi_{obsd} = n_s \cdot \chi_{model} + \chi_0 + \chi_{Curie}$$

where n_s is number of spins per unit cell and χ_0 allows for any discrepancy from the estimated diamagnetic corrections and the temperature independent paramagnetism that may arise from the system which contains low lying excited states. The last term is the Curie contribution due to impurities. The best values are (Table 4):

Since each dimer carries one spin (S=1/2) it is necessary to postulate a dimerization of dimers in order to arrive at a spin dimer model which fits the observed susceptibility data. The room temperature crystal structure determination reveals a regular spacing between dimers, so it would be anticipated that a uniform chain model should be a more appropriate model to describe the magnetic data.[24] To obtain a spin dimer requires an alternation in distances and transfer integrals between dimers. This may happen at a temperature lower than the one at which the crystal structure was determined. However, since there are two dimers per layer per unit cell, it is not required that any of the lattice parameters double.

The EPR spectra do not display any doublet that will be expected from triplet excitons due to the $|\pm1\rangle\leftrightarrow|0\rangle$ transitions or from second order $|+1\rangle\leftrightarrow|-1\rangle$ effects at every temperature and orientation of the samples.[25] The reason may be that the zero-field splitting in the triplet state is very small,

###The reviewer pointed out that the donor arrangement of the present salts is the same as that of (BEDT–TTF)$_2$[Cu$_5$I$_6$], which behaves as a metal down to helium tempearures (see: R. Shibaeva et al., *Krystallografiya*, **33**, 408 (1988).

Table 4.

	η-(BEDT–TTF)$_2$[Ag(CN)$_2$]	η-(BEDT–TTF)$_2$[Au(CN)$_2$]
$2J/k_B$ (K)	313±5	315±2
n_s	0.99±0.02	0.98±0.01
S=1/2 Curie tail (%)	0.6±0.05	0.1±0.05
χ_0 (emu mol^{-1})	$1.5\times10^{-5}\pm1.1\times10^{-5}$	$-2.1\times10^{-5}\pm3.8\times10^{-6}$

though the separation between the two spins is 11 Å (1/2 the *c*-axis). The linewidth of the resonance is broad due to dipolar interaction between molecules and thus may also obscure any triplet state splitting.

Conclusion. In summary, the magnetic susceptibilities of η-(BEDT–TTF)$_2$M(CN)$_2$, is modelled by a singlet–triplet activated system for the first time in the family of BEDT–TTF salts. The transfer integrals and the crystal structure agree with the magnetic model and the observed electrical conductivity, while the tight binding band structure predicts a metallic delocalized ground state. The low resistivities and activation energy suggest weak interactions between the dimers resulting in a small electronic bandwidth.

This work was supported by EPSRC, CNRS, British Council (Alliance programme), and EU (Human Capital and Mobility Programme (Network on Molecular Superconductors)). MK thanks The British Council and Monbusho for a grant to stay at Japan Advanced Institute of Science and Technology at Hokuriku. Prof. Y. Iwasa is thanked for critical discussions.

Appendix

Supplementary Materials deposited at the Cambridge Crystallographic Data Base

Figure: Numbering scheme adopted for of η-(BEDT–TTF)$_2$[Ag(CN)$_2$].

Table 1: Fractional atomic coordinates and thermal factors of η-(BEDT–TTF)$_2$[Ag(CN)$_2$].

Table 2: Bond distances and angles η-(BEDT–TTF)$_2$[Ag(CN)$_2$] at 295 K.

Table 3: List of observed and calculated structure factors for η-(BEDT–TTF)$_2$[Ag(CN)$_2$] at 295 K.

References

1) M. Kurmoo, D. R. Talham, K. L. Pritchard, P. Day, A. M. Stringer, and J. A. K. Howard, *Synth. Met.*, **27**, A177 (1988).

2) a) "Organic Superconductors," ed by T. Ishiguro and K. Yamaji, Springer Verlag, Berlin (1990); b) "Organic Superconductivity," ed by V. Z. Kresin and W. Little, Plenum, New-York (1990); c) "Organic Superconductors (including Fullerenes)," ed by J. M. Williams, J. R. Ferraro, R. J. Thorn, K. D. Carlson, U. Geiser, H. H. Wang, A. M. Kini, and M. -H. Whangbo, Prentice Hall, New York (1992); d) see for example: "Proceedings of the International Conference on Synthetic Metals," "Synthetic Metals," Vols. 19 (1987), 27 (1989), 42 (1991), 56 (1993), and 71 (1995).

3) M. Kurmoo, P. Day, A. M. Stringer, J. A. K. Howard, L. Ducasse, F. L. Pratt, J. Singleton, and W. Hayes, *J. Mater. Chem.*, **3**, 1161 (1993).

4) E. Amberger, H. Fuchs, and K. Polborn, *Synth. Met.*, **19**, 605 (1987).

5) U. Geiser, H. H. Wang, L. E. Gerdom, M. A. Firestone, L. M. Sowa, M. H. Whangbo, and J. M. Williams, *J. Am. Chem. Soc.*, **107**, 8305 (1985).

6) a) M. Kurmoo, K. Pritchard, D. Talham, P. Day, A. M. Stringer, and J. A. K. Howard, *Acta Crystallogr., Sect. B*, **B46**, 348 (1990); b) H. Mori, I. Hirabayashi, S. Tanaka, T. Mori, Y. Murayama, and H. Inokuchi, *Synth. Met.*, **42**, 2255 (1991).

7) J. Larsen and C. Lenoir, *Synthesis*, **2**, 134 (1988).

8) C. J. Gilmore, *J. Appl. Crystallogr.*, **17**, 14 (1984).

9) a) L. Ducasse, A. Abderrabba, J. Hoarau, M. Pasquer, B. Gallois, and J. Gaultier, *J. Phys. C, Solid State Phys.*, **19**, 3805 (1986); b) R. J. Hoffmann, *J. Chem. Phys.*, **39**, 1397 (1963); c) A. Fritsch and L. Ducasse, *J. Phys. (France)*, **1**, 855 (1991).

10) L. Ducasse and A. Fritsch, *Solid State Commun.*, **91**, 201 (1994).

11) U. Geiser, H. H. Wang, K. S. Webb, M. A. Firestone, M. A. Beno, and J. M. Williams, *Acta Crystallogr.*, **43**, 996 (1987).

12) M. Kurmoo, P. Day, P. Guionneau, J. Gaultier, D. Chasseau, L. Ducasse, M. L. Allan, I. D. Marsden, and R. H. Friend, *Inorg. Chem.*, (1995), submitted.

13) J. M. Williams, M. A. Beno, H. H. Wang, U. W. Geiser, T. J. Emge, P. C. W. Leung, G. W. Crabtree, K. D. Carlson, L. J. Azevedo, E. L. Venturini, J. E. Schirber, J. F. Kwak, and M. -H. Whangbo, *Physica B*, **B136**, 371 (1986).

14) T. Mallah, C. Hollis, S. Bott, M. Kurmoo, P. Day, M. L. Allan, and R. H. Friend, *J. Chem. Soc., Dalton Trans.*, **1990**, 859.

15) H. Mori, S. Tanaka, T. Mori, and Y. Murayama, *Bull. Chem. Soc. Jpn.*, **68**, 1136 (1995).

16) I. D. Parker, R. H. Friend, M. Kurmoo, and P. Day, *J. Phys.: Condens. Matter*, **1**, 5681 (1989).

17) T. Sugano, G. Saito, and M. Kinoshita, *Phys. Rev. B; Condens. Matter*, **B34**, 117 (1986).

18) F. L. Pratt, W. Hayes, M. Kurmoo, and P. Day, *Synth. Met.*, **27**, A439 (1988).

19) a) J. M. Williams, A. J. Schultz, H. H. Wang, K. D. Carlson, M. A. Beno, T. J. Emge, U. Geiser, M. E. Hawley, and K. E. Gray, *Physica B*, **143B**, 346 (1986); b) G. Saito, H. Urayama, H. Yamochi, and K. Oshima, *Synth. Met.*, **27**, A331 (1988).

20) a) P. Guionneau, M. Rahal, G. Bravic, J. Gaultier, J. M. Mellado, D. Chasseau, L. Ducasse, M. Kurmoo, and P. Day, *J. Mater. Chem.*, **5**, 1639 (1995); b) M. A. Beno, M. A. Firestone, P. C. W. Leung, L. M. Sowa, H. H. Wang, and J. M. Williams, *Solid State Commun.*, **57**, 735 (1986); c) E. Amberger, H. Fuchs, and K. Polbron, *Angew. Chem.*, **25**, 729 (1986); d) D. Chasseau, J. Gaultier, G. Bravic, L. Ducasse, M. Kurmoo, and P. Day, *Proc. R. Soc. London A*, **442**, 207 (1993).

21) M. Bousseau, L. Valade, M. F. Bruniquel, P. Cassoux, M. Garbauskas, L. Interrante, and J. Kasper, *Nouv. J. Chem.*, **8**, 3 (1984).

22) a) S. D. Obertelli, R. H. Friend, D. R. Talham, M. Kurmoo, and P. Day, *J. Phys.: Condens. Matter*, **1**, 5671 (1989); b) M. Kurmoo, M. A. Green, P. Day, C. Bellitto, and G. Staulo, *Synth. Met.*, **55—57**, 2380 (1993), and unpublished results.

23) B. Bleaney and K. D. Bowers, *Proc. R. Soc. London A*, **214**, 451 (1952).

24) a) J. C. Bonner and M. E. Fisher, *Phys. Rev., A*, **A135**, 640 (1964); b) J. W. Hall, W. E. Marsh, R. R. Weller, and W. E. Hatfield, *Inorg. Chem.*, **20**, 1033 (1981).

25) Z. G. Soos and S. R. Bondeson, in "Linear Chain Compounds," Vol. 3, 193 (1983).